Astron. Astrophys. 324, 699–703 (1997)

ASTRONOMY AND ASTROPHYSICS

The Paschen decrement as a density indicator in MWC349⋆

C. Thum and A. Greve

Institut de Radio Astronomie Millimetrique, Domaine Universitaire de Grenoble, F-38406 St. Martin-d'Hères, France

Received 10 October 1996 / Accepted 7 February 1997

Abstract. We present new observations of the Paschen series hydrogen recombination lines in the circumstellar shell of MWC349. We find the Paschen decrement to be characteristic of a very high density plasma, $n_e \sim 10^8$ cm^{-3}, indicating the origin of the higher quantum number Paschen lines in the dense corona of the circumstellar disk.

The strength of the masing hydrogen recombination α-lines detected previously in the high density plasma of this source is strongly dependent on n_e, since the n_e for maximum amplification increases systematically for decreasing quantum numbers n. The absence of gas with n_e significantly higher than 10^8 cm^{-3} implies that the strength of recombination α-line masers may peak near n = 20 (λ = 400 μm) and that the shorter wavelength transitions may mase only at reduced efficiency.

The good agreement over a large range of n between the observed and the theoretical Paschen decrement shows that any departure from standard recombination theory, possibly due to the strong IR radiation field of the circumstellar disk, must be small.

Key words: recombination lines – stellar envelopes – young stellar objects – circumstellar disks – stars: individual: MWC349

1. Introduction

The circumstellar environment of the peculiar emission line star MWC349 consists of the two principal components: (i) a dense and mainly neutral disk of $\sim$ 300 a.u. extent, and (ii) an ionized wind expanding at constant velocity out to much larger distances. The large and dense ionized shell makes MWC349 one of the strongest radio stars (Altenhoff et al. 1994); it was the first star where radio recombination lines were detected (Altenhoff et al. 1981) and some of them were later found to be masing (Martín-Pintado et al. 1989). To date many recombination lines have been observed at optical and near-IR wavelengths (Thompson et al. 1977; Hamann & Simon 1986,1988; Kelly et al. 1994), as well as in the radio and mm/submm range (Thum et al. 1995 and references therein).

These observations show that recombination lines are emitted by both circumstellar components, demonstrating that a plasma of very high electron density exists close to the disk. The highest electron densities, $n_e = (3-8) \cdot 10^7$ cm^{-3}, were found for the plasma where the recombination line maser originates. These masers which turn on near quantum numbers n = 36 ($\lambda \sim$ 2 mm) tend to become stronger with decreasing n. Since lower n masers need progressively higher n_e for optimum gain (Thum et al. 1992b; Strelnitski et al. 1996), the maximum n_e occuring in the ionized shell is therefore a key parameter for determining the incompletely known range of n over which recombination line masing exists.

In this paper we demonstrate that the Paschen decrement, i.e. the systematic flux variation of the higher order members of the Paschen series (transitions $n \rightarrow 3$, designated Pa(n)), can be used as an indicator of the electron density. The method which exploits the well known feature that the hydrogen level populations thermalize at smaller n for increasing densities, is discussed in Sect. 3.1. Compared to the Balmer series which may be used for the same purpose, the Paschen series is easier to observe in sources of high extinction like MWC349, and possibly most young stellar objects. At the same time, the Paschen series is located at a wavelength range which is easily accessible for ground based spectroscopic observations.

In Sect. 3.2 we discuss our data of MWC349 together with observations of the classical HII region M 17 which we have obtained with the same instrumentation as a test of the method. We show that our MWC 349 data are in very good agreement with the only existing similar investigation (Hamann & Simon 1988). This agreement stimulated the more detailed analysis presented here of the available Paschen decrement data.

2. Observations

The observations were made on 14 July 1993 with the ESO 1.5 m telescope, La Silla, Chile, equipped with a Boller & Chivens Cassegrain spectrograph and a 600 lines/mm grating (#28) and CCD detector (Ford 24). This configuration recorded in first order a spectral range of $\sim$ 6500 - 9700 Å at 2 Å/pixel, equivalent to an effective spectral resolution of $\lambda/\Delta\lambda \sim$ 4000. Dur-

Send offprint requests to: C. Thum

⋆ Based on observations collected at ESO, La Silla, Chile.

ing the observation the seeing was $\sim 1''$, or better, and the sky transparancy was excellent. The $5'$ long slit was centered on MWC 349 and, in M 17, on the stars #1 and #3 (Chini et al. 1980). Immediately after the exposures of each of our sources, MWC 349 and M 17, a standard star was observed near the respective target source. The DA-type standard star EG 274 (Baldwin & Stone 1994) was used for MWC 349 and LTT 7379 for M 17. Sky subtraction and calibration were made as in previous observations (Greve et al. 1991, 1994) where the same telescope - spectrograph combination was used.

Owing to the low atmospheric extinction (~ 0.015 mag/air mass) in the wavelength range of 8000 - 9000 Å and to the small time and elevation difference between target and standard stars, we estimate our flux calibration to be accurate to 20%. Differences between our measurement of the Pa(9) line flux (Table 1) and previous observations (Hamann & Simon 1986; Kelly et al. 1994) are of this order. Relative calibration is probably accurate to 10%, since sufficient signal to noise was obtained for all lines discussed here.

Our spectrogram covers the Paschen series from n = 6 to the series limit near 8206 Å. We do not consider lines $n < 8$ because of insufficient exposure of the standard star at the red end of the sensitivity range. Similarly, line fluxes for $n > 28$ are too uncertain due to merging of neighbouring members of the Paschen series. The Paschen lines in between these limits are listed in Table 1, normalized to the flux of Pa(9). In order to facilitate comparison with previous observations these ratios have not been corrected for extinction which is A_V= 10 mag for MWC 349 (Cohen et al. 1985) and A_V= 2 mag for the field selected in M 17 (Chini et al. 1980).

In the line-rich source MWC 349 the accuracy of the Paschen line ratios is clearly limited by line blends. Severe cases where the Paschen line flux may be affected by more than 10% are noted in Table 1. Most of these blends were already identified in the echelle spectrum obtained by Hamann & Simon (1986). In a spectrum of even higher resolution[1] (Hamann & Simon, private communication) most of the lines were resolved and the magnitude of most of the blends could be assessed quantitatively. We did not detect Paschen lines in absorption as would be expected from the photosphere of a normal, hot, main-sequence star. The absence of photospheric lines in MWC 349 was noted before by Cohen et al. (1985).

Table 1. Observed Paschen line ratios (transitions $n \rightarrow 3$).

n	Wavelength (Å)	log [Pa(n)/Pa(9)] MWC 349	M 17	note
8	9546	0.51	0.23	
9	9229	0.00	0.00	a)
10	9015	-0.16	-0.13	
11	8863	-0.29	-0.31	
12	8750	-0.38	-0.40	
13	8665	-0.40	-0.53	b)
14	8598	-0.56	-0.59	
15	8545	-0.52	-0.74	b)
16	8502	-0.64	-0.83	b)
17	8467	-0.73	-0.87	
18	8438	–	-0.97	c)
19	8413	-1.01	-1.04	
20	8392	-1.08	-1.09	
21	8374	-1.14	-1.10	
22	8359	-1.02	-1.08	b)
23	8346	-1.22	-1.24	
24	8333	-1.33	-1.29	
25	8323	-1.44	-1.44	
26	8314	-1.52	-1.45	
27	8306	-1.42	-1.50	
28	8298	-1.58	-1.75	

a) Pa(9) line flux in MWC 349: $9 \cdot 10^{-12}$ erg s^{-1}cm^{-2}.
b) transition weakly blended in MWC 349, see also Hamann & Simon (1988) for possible line identifications.
c) very strong blend in MWC 349. line of MWC 349 free of conspicuous blend.

3. Results

3.1. Theoretical Paschen decrement

In view of strong arguments indicating very high optical depths in the near-IR transitions of He I (Thompson et al. 1977), we adopt Case B in the following discussion. Quantitatively, the Paschen decrement is a function of density n_e and temperature T_e. We calculated the line ratios Pa(n)/Pa(9) of the Paschen series using the hydrogen recombination line emission coefficients tabulated by Storey & Hummer (1995). We find that the ratios Pa(n)/Pa(9) depend very little on T_e, less than $\sim 20\%$ for values T_e = 5000 - 15000 K as encountered in circumstellar envelopes. We have thus adopted for MWC 349 a homogeneous temperature T_e = 7500 K which is close to measured values (White & Becker 1985; Martín-Pintado et al. 1989). In Fig. 1 we plot the ratios Pa(n)/Pa(9) for densities n_e in the range from 10^2 to 10^{14} cm^{-3}. The curves are contained between two asymptotes and show a significant dependence of the line ratios on n_e which may reach a factor 3 to 4 between low and high densities. The two asymptotes represent extreme values of the b_n coefficients, i.e. the maximum value b_n = 1 at high densities where collisions dominate the level populations, and minimum values b_n = 0.2...0.3 (for the quantum number range considered here) at low densities where radiative transitions dominate. For increasing n_e, the transition from the collisional to the radiative domain occurs at successively lower quantum numbers. It is this behaviour which makes the Paschen decrement a useful diagnostic tool for determination of n_e in dense plasmas.

3.2. Observed Paschen decrement

For M 17 and MWC 349 we plot in Fig. 2 the observed (not corrected for reddening) line ratios of the Paschen series. For MWC 349 we show in addition to our data (Table 1) the ob-

[1] An echelle spectrum with a resolution of ~ 11000 was obtained at the Kitt Peak National Observatory by Hamann and Simon, and was kindly made available to us.

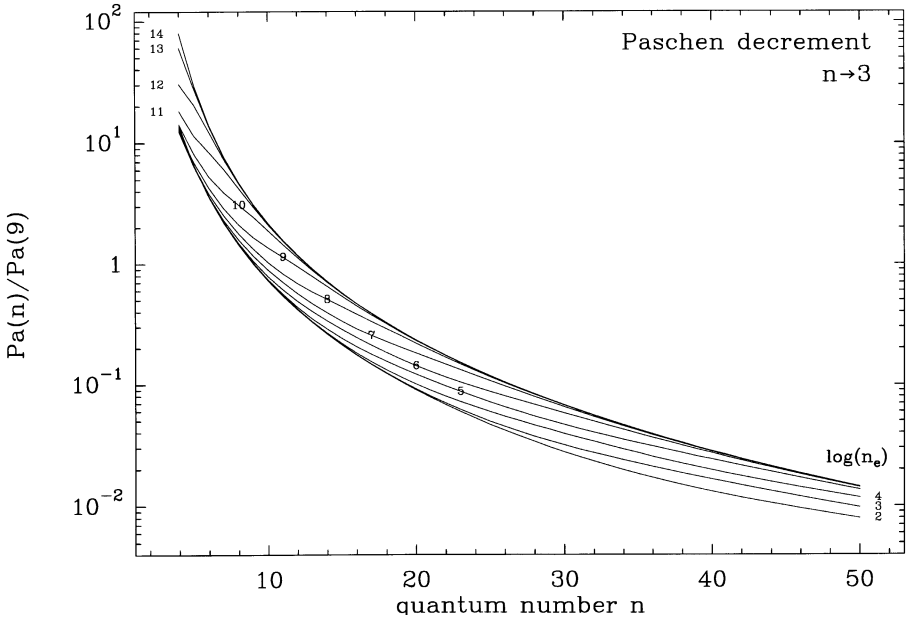

Fig. 1. Theoretical Paschen decrement (Case B) for T_e= 7500 K without extinction (A_V = 0). The curves are parameterized with log(n_e) and normalized to the Pa(9) emission coefficient for low density (log n_e = 2). The line emission coefficients are from Storey & Hummer (1995).

servations of Hamann & Simon (1988) and Kelly et al. (1994). Unfortunately, no complemetary data for $n < 8$ seem to exist for M 17. The observations are normalized to the Pa(9) transition which was included in all data sets.

The different data sets of MWC 349 agree surprisingly well where they overlap, with the possible exception of Pa(8). We note that MWC 349 is variable in many parts of the electromagnetic spectrum, typically by a factor ~ 4 (Gottlieb & Liller 1978; Andrillat et al. 1982; Thum et al. 1992a). Variability may thus account for some differences in these data sets which were not observed at the same time. The line Pa(18) of our observation is omitted because of a strong blend; some lines are not available in the Hamann & Simon data because they coincide with echelle order separations. Some other lines, which are marked as possible blends in Table 1, tend to lie high in Fig. 2. There exists a small, but systematic discrepancy with increasing n between our data and those of Hamann & Simon. We attribute this difference to the difficulty in determining the continuum level near the series limit. This difficulty, slightly worse for our lower resolution spectrogram, leads to an underestimation of the line fluxes at high n.

We also plot in Fig. 2 the theoretical Paschen decrements, with appropppriate reddening applied, for a typical low density plasma of $n_e = 10^3$ cm^{-3} (continuous line) and for a high density plasma of $n_e = 10^8$ cm^{-3} (dashed line). We adopted a reddening law of the form $A_\lambda \sim \lambda^{-1.85}$ (Landini et al. 1984; Cardelli et al. 1989), together with visual extinctions of A_V= 2 mag for M 17 (Chini et al. 1980) and of A_V= 10 mag for MWC 349 (Cohen et al. 1985). The reddened decrements are normalized to Pa(9) as for the observational data.

In M 17, the solid line fits the observation well, suggesting a low average electron density in this classical HII region, rather similar to the values near 10^3 cm^{-3} which are derived from radio continuum observations (Berulis & Sorochenko 1973; Schraml & Mezger 1969). However, for MWC 349 the low density decrement is inadequate by a factor $\gtrsim 2$ for $n \geq 10$, and a reasonable fit can only be obtained with the high density decrement of $n_e = 10^8$ cm^{-3}. At such high densities, the theoretical decrement turns rather sharply from the low density asymptote to the high density one, thus allowing a surprisingly precise determination of n_e. We estimate that the margin of n_e permitted by the fit is at most a factor 10.

We conclude that the bulk of the Paschen line emission in MWC 349 originates in a plasma of density $n_e \sim 10^8$ cm^{-3}, much higher than the 10^6 cm^{-3} fit shown in Fig. 3 of Hamann & Simon. There is no evidence of a plasma of significantly (factor 3 or more) higher density.

4. Discussion

4.1. Maximum plasma density

The star MWC 349 is the source of an intense ionized stellar wind. Its radio continuum energy distribution shows the classical $\nu^{0.7}$ frequency dependence (Altenhoff et al. 1994) which indicates an outflow of constant velocity. This frequency dependence implies a density stratification of the ionized shell of $n_e \sim 1/r^2$. The radial extent over which this density law applies can be derived from the frequency range of the $\nu^{0.7}$ section of the spectral energy distribution (Panagia & Felli 1975). At low frequencies the $\nu^{0.7}$ spectrum extends to 1.4 GHz (White & Becker 1985) indicating an outer radius of the ionized wind of $\sim 10^4$ a.u. and $n_e \sim 300$ cm^{-3}. At high frequencies the $\nu^{0.7}$ spectrum continues into the far-IR (Harvey et al. 1979) where it merges with the long wavelength emission of the hot dust in the circumstellar disk.

The high frequency turn-over of the wind spectrum, and thus the maximum electron density n_e^{max}, are presently unknown. However, it cannot be smaller than 10^8 cm^{-3}, the density where the highest frequency recombination line masers (quan-

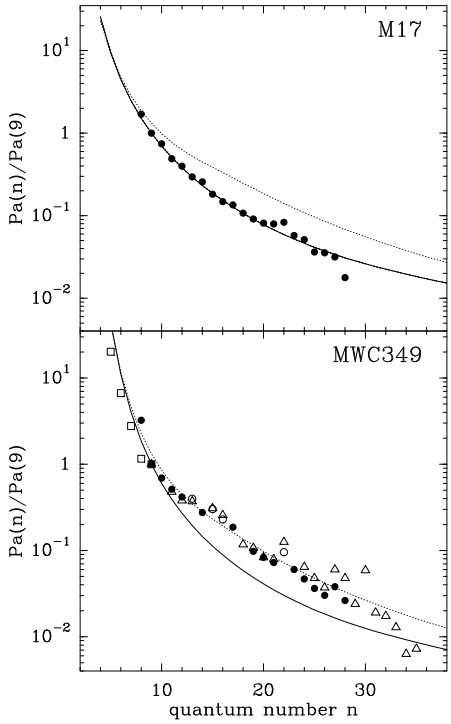

Fig. 2. Paschen decrements observed in M 17 (top) and MWC 349 (bottom). The data are from this paper (•; ○ for blends), from Hamann & Simon (1988) (△), and from Kelly et al. (1994) (□). The lines represent theoretical decrements for case B and T_e= 7500 K. Continuous lines refer to the electron density of $n_e = 10^3$ cm^{-3}, dashed lines to $n_e = 10^8$ cm^{-3}. A wavelength dependent reddening (see text) has been applied to these curves.

tum number n = 21 at 453 μm) are thought to operate (Thum et al. 1992b; 1994). Our present estimate of $n_e^{max} \approx 10^8$ cm^{-3} derived above is therefore compatible with the existing millimeter and submillimeter wavelength maser observations.

The existence of this n_e^{max} may directly affect the recombination line masers possibly operating at even shorter wavelengths. These IR transitions require electron densities progressively higher than 10^8 cm^{-3} for maximum gain per unit length (Strelnitski et al. 1996). Since these higher densities do not occur, we predict that the IR transitions, contrary to their mm/submm counterparts, mase at progressively *reduced* efficiency with decreasing wavelength. We then expect the maximum of the maser line flux to occur near quantum numbers $n \approx 20$.

4.2. The disk corona

Considerable evidence suggests that the high density plasma where the recombination line masers originate is associated with the circumstellar disk (Gordon 1992; Planesas et al. 1992; Thum et al. 1992a). This seems to imply that also the high density plasma emitting the Paschen lines originates on the disk. We quantify the emission stratification of the flux F_L in a Paschen line by introducing the volume emission measure EM = $\int n_e^2 4\pi r^2\, dr$. F_L is then proportional to the product of the line emissivity $\epsilon(n)$ and EM. If we decompose the plasma of the constant-velocity wind into concentric spherical shells, the line flux dF_L from these shells is proportional to $1/r^2$. The largest contribution to F_L therefore comes from the innermost shell where the density is highest. We identify this shell with the plasma close to the neutral disk, i.e. the disk corona. It is therefore not surprising that the observed Paschen decrement can be well reproduced by only one, seemingly homogenous, high density shell.

We must expect, however, that spherical symmetry breaks down near the disk. In the general case where the variation of n_e with r is not known, we may still assume that F_L is dominated by the most dense regions. This is due to the monotonic increase of $\epsilon(n)$ with n_e. Consider the idealized case of two emission regions of equal volume emission measure, but different n_e, say 10^3 and 10^8 cm^{-3}. For quantum numbers $n < 10$, $\epsilon(n)$ is the same for the two regions, and they contribute equally to the total F_L. For $n \geq 18$, $\epsilon(n)$ is a factor ~ 3 higher in the high density region which then dominates the total line emission. We conclude that the higher n transitions of the Paschen series are probably more weighted by emission from the disk corona than the low n transitions. We would then expect the high n Paschen lines to be more clearly double-peaked owing to the disk rotation than the low n lines, an effect which may have been detected already (Hamann & Simon 1988).

4.3. Departure from standard recombination theory ?

Hummer & Storey (1992) have investigated several effects which could cause departures of the hydrogen level population from the case B values. The physical parameters charaterizing MWC 349, i.e. those of a dense stellar envelope, are certainly different from those of H II regions as studied by these authors. In particular, we believe that the influence of dust radiation may be stronger in MWC 349 than considered by them. From the models investigated (dust temperatures of 100 K, $n_e = 10^2$, 10^4 cm^{-3}) they find departures from case B populations of the order of only 10%. It would be informative to calculate models closer to the parameters of MWC 349, namely for dust temperatures of at least 850 K (Harvey et al. 1979) and considerable dust optical depth. Using this temperature, the observed size of $\sim$ 60 mas of the dust source (Leinert 1986), and the continuum flux density of 150 Jy observed near its spectral maximum at $\sim 10\mu$ (Aitken et al. 1990; Herzog et al. 1980), we derive a 10μ dust optical depth of $\sim$ 0.3. This high value sets MWC 349 clearly apart from HII-regions where mid-IR dust optical depths are normally much smaller, and thus emphasizes the increased significance of the mid-IR radiation field for the hydrogen level populations.

From the rms difference between our observations and the best fit theoretical curve we derive an upper limit of 12% for the departure from case B (dashed line in Fig. 2). The true upper limit may be somewhat smaller if lines suspected to be weak blends are left out of the rms calculation. Any perturbation of the b_n coefficients by the IR radiation field should be smaller than this limit. We consider the agreement between the theory and the

observations very satisfactory, especially in view of the crude model of density stratification used in the above discussion.

5. Conclusions

We present new observations of the Paschen series in MWC 349 and M 17 which we use, in connection with published data, to determine the Paschen decrements with high precision over an unprecedented large range of quantum numbers. While for M 17 the observed decrement is fully compatible with a low average value of the electron density $n_e \sim 10^3$ cm^{-3} known from radio and optical observations, the Paschen decrement observed in MWC 349 clearly requires much higher densities. The theoretical decrement for $n_e = 10^8$ cm^{-3}, with reddening applied, fits the observations very well, with an rms residual of 12%, which is of the order of the observational error.

This remarkably good fit shows in a simple manner the transition of the hydrogen level population coefficients b_n from the collision dominated to the radiative domain, and demonstrates the validity of the recombination theory in the special conditions encountered in MWC 349. In particular, the influence of the intense IR radiation field from the dust in the circumstellar disk on the b_n coefficients must be small compared to observational errors.

Our fit to the Paschen decrement in MWC 349 suggests that the maximum of the electron density is near 10^8 cm^{-3} and that it occurs in the disk corona. This implies that recombination line masers at quantum numbers $n \leqq 20$ (wavelengths $\leqq 400\mu$m) operate at reduced gain, and they should therefore cease to exist at quantum numbers not much lower than this.

As n increases, progressively larger fractions of a Paschen line originate in the highest density plasma of the disk corona. Their line profile should then become progressively more double-peaked due to disk rotation. This effect may have already been detected (Hamann & Simon 1986), but should be confirmed with spectra of more adequate resolution.

In summary, we find that observations of the Paschen series are a sensitive tool for measuring electron densities in high density stellar envelopes. This novel tool is particularly sensitive to high electron densities as characteristic of a disk corona. With sufficiently high spectral resolution, the presence of a circumstellar disk may be inferred directly.

Acknowledgements. We thank the staff of ESO, and in particular Mr. H. Vega, for assistence with the observations. Drs. F. Hamann and M. Simon have generously made available to us their unpublished high resolution echelle spectrum of MWC 349. Fruitful discussions with Drs. D. Downes, V. Strelnitski, and M. Walmsley are gratefully acknowledged. We also thank the referee, Dr. Storey, for comments. The tabulated recombination line emission coefficients (Storey & Hummer 1995) were obtained from the Centre des Données, Strassbourg.

References

Aitken D.K., Smith C.H., Roche P.F., Wright, C.M. 1990, MNRAS 247, 466
Altenhoff W.J., Strittmatter P.A., Wendker H.J. 1981, A&A 93, 48
Altenhoff W.J., Thum C., Wendker H.J. 1994, A&A 281, 161
Andrillat Y., Ciatti F., Swings J.P. 1982, Ap&SS 83, 423
Baldwin J.A., Stone R.P.S. 1994, M.N.R.A.S. 206, 241
Berulis I.I, Sorochenko R.L. 1973, Sov. Astron. 17, 179
Cardelli J.A., Clayton G.C., Mathis J.S. 1989, ApJ 345, 245
Chini R., Elsässer H., Neckel Th. 1980, A&A 91, 186
Cohen M., Bieging J.H., Dreher J.W., Welch W.J. 1985, ApJ 292, 249
Gordon M. A. 1992, ApJ 387, 701
Gottlieb E.W., Liller W. 1978, ApJ 225, 488
Greve A., Castles J., McKeith C.D. 1991, A&A 251, 575
Greve A., Castles J., McKeith C.D. 1994, A&A 284, 919
Hamann F., Simon M. 1986, ApJ 311, 909
Hamann F., Simon M. 1988, ApJ 327, 876
Harvey P.M., Thronson H.A. 1979, ApJ 231, 115
Hummer D.G., Storey P.J. 1992, MNRAS 254, 254
Herzog A.D., Gehrz R.D., Hackwell J.A. 1980, ApJ 236, 189
Kelly D.M., Rieke G.H., Campell B. 1994, ApJ 425, 231
Landini M., Natta A., Oliva E., Salinari P., Moorwood, A.F.M. 1984, A&A 134, 284
Leinert C. 1986, A&A 155, L6
Martín-Pintado J., Bachiller R., Thum C., Walmsley C. M. 1989, A&A 215, L13
Panagia N., Felli M. 1975, A&A 39, 1
Planesas P., Martín-Pintado J., Serabyn E. 1992, ApJ 386, L23
Schraml J., Mezger P.G. 1969, ApJ 156 269
Storey P.J., Hummer D.G. 1995, MNRAS 272, 41
Strelnitski V.S., Ponomarev V.O., Smith H.A. 1996, ApJ 470, 1118
Thompson, R.I., Strittmatter, P.A., Erickson, E.F., et al. 1977, ApJ, 218, 170
Thum, C., Martín-Pintado, J., Bachiller, R. 1992a, A&A, 256, 507
Thum, C., Matthews, H.E., Martín-Pintado, J., et al. 1992b, A&A 283, 582
Thum, C., Matthews, H. E., Harris, A. H., et al. 1994, A&A 288, L25
Thum C., Strelnitski V.S., Matthews H.E., Martín-Pintado J., Smith H.A. 1995, A&A, 300, 843
White, R.L., Becker, R.H. 1985, ApJ, 297, 677

This article was processed by the author using Springer-Verlag LaTeX A&A style file *L-AA* version 3.